Residual and fracture strains of Bi2223 filaments and their relation to critical current under applied bending and tensile strains in Bi2223/Ag/Ag alloy composite superconductor

AUTHOR(S):

Ochiai, S; Shin, JK; Iwamoto, S; Okuda, H; Oh, SS; Ha, DW; Sato, M

JOURNAL OF APPLIED PHYSICS **103**, 123911 (2008)

Residual and fracture strains of Bi2223 filaments and their relation to critical current under applied bending and tensile strains in Bi2223/Ag/Ag alloy composite superconductor

S. Ochiai,[1,a)] J. K. Shin,[1] S. Iwamoto,[1] H. Okuda,[1] S. S. Oh,[2] D. W. Ha,[2] and M. Sato[3]
[1]*Department of Materials Science and Engineering, Graduate School of Engineering, Kyoto University, Sakyo-ku, Kyoto 606-8501, Japan*
[2]*Korea Electrotechnology Research Institute, 28-1 Sungju-Dong, Changwon 641-120, Republic of Korea*
[3]*Japan Synchrotron-Radiation Research Institute (JASRI), Kohto, Sayo 679-5198, Japan*

(Received 1 February 2008; accepted 20 April 2008; published online 25 June 2008)

Mechanical and electromagnetic stresses are exerted on Bi2223/Ag/Ag alloy superconducting composite tapes during fabrication/winding and operation, which cause reduction in critical current when the Bi2223 filaments are damaged. In the damage process, the thermally induced residual strain and fracture strain of the Bi2223 filaments play a dominant role. The aim of the present work was to propose a comprehensive method for estimation of these strain values and a quantitative description method of the relation of critical current to the applied bending/tensile strain, and to examine the accuracy of the method in comparison with the experimental results. The residual strain of Bi2223 filaments in the composite tape was measured by the x-ray diffraction method. The measured residual strain value was used for analysis of the load-strain curve, from which the intrinsic fracture strain of filaments was estimated. The relation of critical current to applied bending/tensile strain was predicted by the proposed calculation procedure, in which the estimated strain values were input. The predicted critical current-applied strain relation agreed well with the experimental results, suggesting that the present method is a useful tool for prediction/description of tensile/bending applied strain dependence of critical current of multifilamentary-type conductors.
 [DOI: 10.1063/1.2948933]

I. INTRODUCTION

As composite superconductor tapes are subjected to bending and tensile stresses during magnet winding and electromagnetic stress (Lorentz force) during operation,[1–3] the relation of deformation and fracture behavior of multifilamentary Bi2223-composite tapes to the superconducting property has been studied widely. It has been revealed that the critical current of the composite tapes under applied tensile/bending strain decreases seriously beyond the irreversible strain due to the damage evolution, and once the applied strain exceeds such an irreversible strain, the critical current never returns to the original value even when the applied strain is released, while it returns reversibly below the irreversible strain.[1–27] For description of damage behavior of Bi2223 filaments that transport superconducting current, two important parameters have been mentioned.[4,13,14,16,19,21,27] One is the intrinsic fracture strain $\varepsilon_{Bi,f}$ and another is the residual strain $\varepsilon_{Bi,r}$. If the Bi2223 filaments are tested alone, they fracture at the intrinsic fracture strain $\varepsilon_{Bi,f}$. In practice, as they are embedded in Ag and the assembly is sheathed with Ag alloy, they have residual strain $\varepsilon_{Bi,r}$ which arises during cooling from the heat-treatment temperature due to the difference in coefficient of thermal expansion among the constituents (Bi2223, Ag, and Ag alloy sheath). The residual strain of Bi2223 filaments is compressive in the current-transportation direction since the coefficient of thermal expansion of Bi2223 is lower than that of Ag and Ag alloy.[4,9,10,13,15,20,21,27] Thus, the fracture of the Bi2223 filaments embedded in the composite tape is retarded by $-\varepsilon_{Bi,r}$ under applied tensile strain. As the fracture strain $\varepsilon_{Bi,f}$ of the Bi2223 filaments is not necessary high (around 0.1%),[4,9,11,13,18,19,21,22,27] the residual strain $\varepsilon_{Bi,r}$ contributes largely to the strain tolerance of critical current of the composite tape.

The aim of the present work is to develop a simple estimation method of the residual and intrinsic tensile fracture strains of Bi2223 filaments in the current-transport direction (sample length direction) and to describe the relation of critical current to bending strain and irreversible tensile strain for critical current with the estimated strain values. The present work consists of the following measurement and analysis.

(1) *Measurement of residual strain $\varepsilon_{Bi,r}$ of Bi2223 filaments in the composite tape at room temperature*. The x-ray diffraction method was used. The result will be presented in Sec. III.

(2) *Estimation of intrinsic fracture strain $\varepsilon_{Bi,f}$ of Bi2223 filaments*. The applied tensile strain at which damage of Bi2223 filaments takes place in the composite tape, corresponding to $\varepsilon_{Bi,f}$-$\varepsilon_{Bi,r}$, was estimated from the load-strain curve at room temperature. In this approach, the feature that the load carrying capacity of the composite tape with fractured Bi2223 filaments is reduced in comparison with that without fractured ones[11,13,21] was used. Combining the estimated $\varepsilon_{Bi,f}$-$\varepsilon_{Bi,r}$ value with the $\varepsilon_{Bi,r}$ value estimated in (1), we obtained $\varepsilon_{Bi,f}$ value, as will be shown in Sec. III.

(3) *Application of the estimated $\varepsilon_{Bi,f}$ and $\varepsilon_{Bi,r}$ values at*

[a)]Electronic mail: shojiro.ochiai@materials.mbox.media.kyoto-u.ac.jp.

room temperature to describe the change of critical current with increasing applied bending strain ε_B of the samples bent at room temperature. In this experiment, the damage was given to the composite tape by bending at room temperature. The bent composite tape was cooled down to 77 K, at which the critical current was measured. The $\varepsilon_{Bi,f}$ and $\varepsilon_{Bi,r}$ values estimated in (1) and (2) were used in the modeling analysis for prediction of the relation of critical current to bending strain. The predicted relation agreed well with the measured one, as will be shown in Sec. IV.

(4) *Calculation of change in residual strain of the constituents (Bi2223, Ag, and Ag, alloy) as a function of temperature between room temperature and* 77 K. The residual strain change in each constituent from room temperature to 77 K was calculated with the rule of mixtures,[27] in which the yielding behavior of Ag was incorporated. The result will be presented in Sec. V.

(5) *Application of the $\varepsilon_{Bi,f}$ and $\varepsilon_{Bi,r}$ values at* 77 K *calculated in (4) to predict the irreversible tensile strain $\varepsilon_{T,irr}$ for critical current at* 77 K. In the experiment, the tensile strain was given to the composite tape at 77 K and critical current was measured also at 77 K. In this case, the sample was damaged at 77 K in contrast to the case of bending where the sample was damaged at room temperature. The irreversible tensile strain $\varepsilon_{T,irr}$ for critical current, being equal to $\varepsilon_{Bi,f}$-$\varepsilon_{Bi,r}$ at 77 K, was predicted from the results of (4) above. The predicted value was close to the experimental one, as will be shown in Sec. V.

As shown later in detail, the approach of the present work was found to be a useful tool for estimation of residual and fracture strains of the filaments, and yield strains of Ag and Ag alloy, and for description/prediction of the irreversible tensile strain of critical current and variation of critical current as a function of bending strain. The application of the present approach is not limited to Bi2223 filamentary tapes. It can be applied also to Bi2212 and MgB_2 multifilamentary tapes and wires in the same manner as in the present work. The procedure and used formulae are simple, which is also a merit in application.

II. EXPERIMENTAL DETAILS

The multifilamentary Bi2223/Ag/Ag alloy composite tape, fabricated at Korea Electrotechnology Research Institute (KERI), was used as the experimental sample. It contained 55 Bi2223 filaments. The thickness and width of the sample were 0.23 and 4.1 mm, respectively. The cross section of the sample is shown in Fig. 1(a). When the thickness direction is three times enlarged from the as-observed one in Fig. 1(a), the region where the Bi2223 filaments that transport the superconducting current are embedded in Ag is clearly found, as surrounded with the broken curve in Fig. 1(b). Such a region is noted as core in this work. When the filaments are damaged, the critical current is reduced. The relation of critical current to the damage evolution, shape of the core, and bending strain will be discussed in Sec. IV.

The thermal history of the present sample is presented in Fig. 2. The sample had been cooled down from the heat-treatment temperature T_H to room temperature [RT(1) in Fig. 2] and then to 77 K (1) for precheck of the critical current at KERI and had been warmed up to room temperature [RT(2)]. At RT(2), the sample was sent from KERI to Kyoto University, at which experiments were carried out. In the measurement of the critical current-bending strain relation, the sample was bent at RT(2) and cooled down to 77 K (2) at which the critical current was measured. In the measurement of the critical current-tensile strain relation, the sample was pulled in tension at 77 K (2) and, subsequently, the critical current was measured at the same temperature of 77 K (2). In this way, the bending damage was given at room temperature and the tensile one at 77 K.

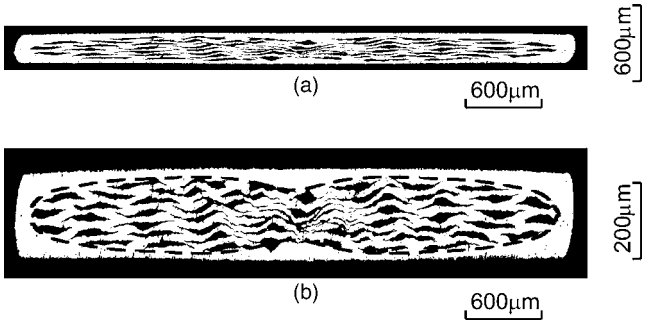

FIG. 1. Transverse cross section of the composite tape. (a) shows the as-observed optical micrograph. (b) shows the modified micrograph, in which the thickness direction is three times enlarged from (a). The broken curve in (b) shows the shape of the core.

In order to estimate the mechanical property values for analysis of residual strain and to estimate the intrinsic fracture strain of Bi2223 filaments in the composite, tensile test was carried out using a universal testing machine (autograph AG-50kNG, Shimadzu, Japan) at a strain rate of 2×10^{-4}/s at room temperature [RT(2)] for a gage length of 25 mm. Tensile strain was applied in the sample length direction (current transport direction). The strain of the composite tape was measured with a very light weight extensometer developed by Nyilas.[17,24] For estimation of the residual strain of Bi2223 filament in the composite at room temperature [RT(2)], in-site strain measurement of Bi2223 filaments in the composite tape under the externally applied tensile strain ε_T of 0–0.08% was carried out at the beam line 46XU of a synchrotron-radiation facility, SPring 8, Japan. The experiment was carried out in a similar manner to our former

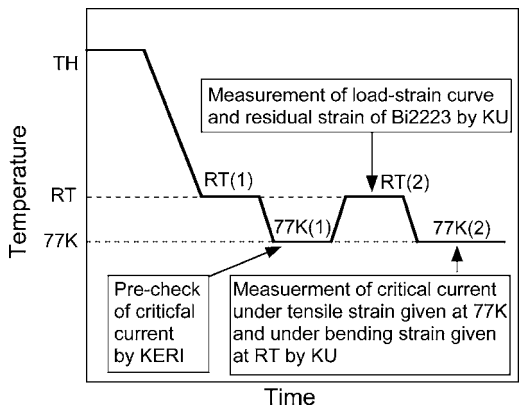

FIG. 2. Thermal history of the sample.

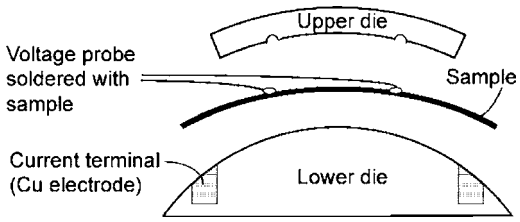

FIG. 3. Bending device.

work.[27] The x-ray from an undulator was monochromatized into a beam of 22 keV and introduced to the sample position. The beam size was 0.5×1.0 mm^2. To prepare the strain-free reference sample, the bare Bi2223 filaments were extracted from the composite tape by etching away the Ag and Ag alloy with a NH_4OH/H_2O_2 solution. The peak positions of the (200) and (220) planes were measured for the strained Bi2223 filaments in the composite as well as for the strain-free extracted ones. From the difference in the peak position between the strained and strain-free Bi2223 filaments, the strain of Bi2223 filaments in the composite was estimated for each plane and the results were averaged. The residual strain $\varepsilon_{\mathrm{Bi,r}}$ of the Bi2223 filaments at RT(2), corresponding to the strain value at $\varepsilon_{\mathrm{T}}=0\%$, was estimated by applying the least square method to the measured relation of $\varepsilon_{\mathrm{Bi}}$ to ε_T.

The measurement of critical current I_c of bent samples was carried out with the procedure employed in the round robin test.[25] In the present work, the bending strain ε_B was given to the sample at RT(2) by pressing the sample with the upper GFRP die to the lower one with the same curvature (Fig. 3). The voltage taps and current terminals were soldered with the bent sample. The bending strain ε_B corresponding to the tensile strain in the sample length direction of the outer surface of the composite in the tensile side, is given by

$$\varepsilon_B = t/(2R), \tag{1}$$

where t is the thickness of the sample (0.23 mm in the present work) and R is the radius of the die. Six pairs of dies with the radius $R=\infty$ (straight dies), 61.6, 34.0, 22.3, 17.3, and 13.8 mm, were used to give bending strain, corresponding to $\varepsilon_B=0$, 0.19%, 0.34%, 0.52%, 0.67%, and 0.83%, respectively. The sample bent at room temperature was cooled down to 77 K [77 K (2) in Fig. 2], at which the critical current I_c was measured by the ordinary four probe method with a criterion of 1 μV/cm in the self-magnetic field. The distance between the voltage taps was 30 mm. After the measurement of the critical current, the sample was warmed up to room temperature. Then the bending strain was raised to the next prescribed one and the sample was again cooled down to 77 K for measurement of critical current. Such a procedure was repeated to obtain the critical current-bending strain relation.

The measurement of the change of critical current I_c of the composite tape under tensile strain was carried out in the following procedure. Both ends of the sample were gripped at room temperature. The gripped sample was cooled down to 77 K [77 K (2) in Fig. 2]. In order to keep the zero strain state of the sample during cooling down, the load induced by the shrinkage of the sample was monitored with a load cell and the location of the cross head was controlled as to keep the monitored load value to be zero. The sample cooled down to 77 K was pulled in tension also at 77 K. The tensile strain ε_T of the sample at 77 K was measured with the Nyilas-type extensometers[17,24] as well as that at room temperature. The applied tensile strain was raised in step of around 0.03%. The critical current was measured in the same manner as that for bent samples.

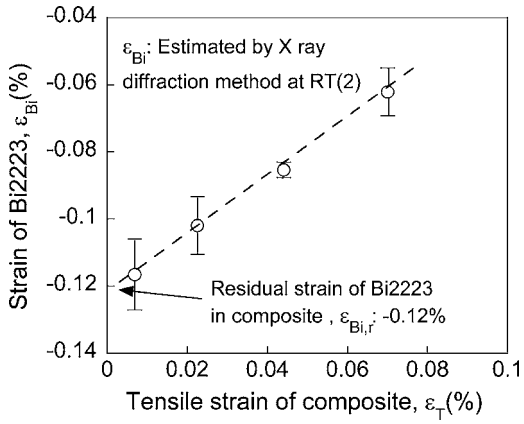

FIG. 4. Change of strain $\varepsilon_{\mathrm{Bi}}$ of Bi2223 filaments with applied tensile strain ε_T at room temperature [RT(2) in Fig. 2], measured with the x-ray diffraction method.

III. RESIDUAL AND FRACTURE STRAINS OF BI2223 FILAMENTS ALONG THE SAMPLE LENGTH AT ROOM TEMPERATURE

Figure 4 shows the change of the strain $\varepsilon_{\mathrm{Bi}}$ of Bi2223 filaments in the composite along the sample length direction with increasing applied tensile strain ε_T at room temperature [RT(2) in Fig. 2], measured by the x-ray diffraction method. From the regression analysis of the measured $\varepsilon_{\mathrm{Bi}}$-$\varepsilon_T$ relation and extrapolation to $\varepsilon_T=0$, the residual strain $\varepsilon_{\mathrm{Bi},r}$ of Bi2223 at RT(2) was estimated to be −0.12%.

Figure 5(a) shows the tensile load (L_c)-strain (ε_T) curve of the composite at room temperature [RT(2)]. It is noted that we need not convert the load-strain curve to stress-strain one for the present purpose. We can use directly the measured load-strain curve to estimate various mechanical parameter values necessary for calculation as follows. The curve is characterized by the following three regions.[13,27]

(1) region I: Bi2223, Ag and Ag alloy deform elastically;
(2) region II: Bi2223 and Ag alloy deform elastically, while Ag deforms plastically;
(3) region III: Bi2223 deforms elastically, while Ag and Ag alloy deform plastically.

The strain hardening coefficient of metal is, in general, far lower than the Young's modulus. Noting the Young's modulus as E and cross-sectional area as A, the Young's modulus of the composite tape in each region is approximately expressed by[13,27,28]

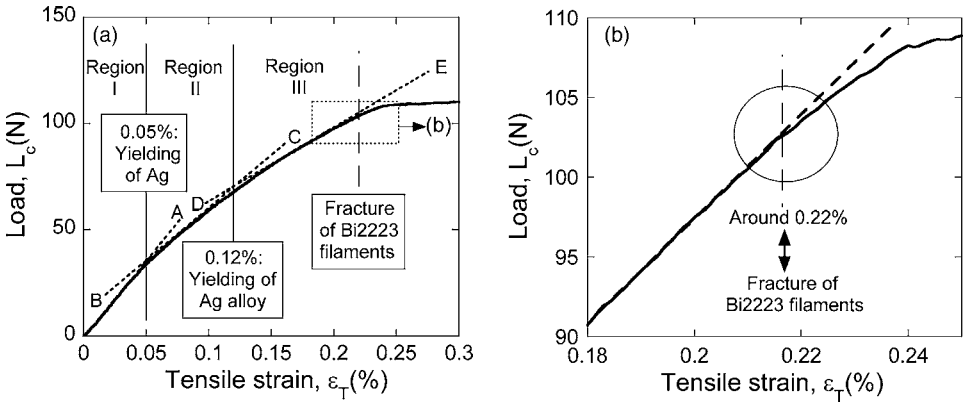

FIG. 5. Measured tensile load-strain curves of the composite tape at room temperature [RT(2)]. The region surrounded by the rectangle in (a) is presented at high magnification in (b). The open circle in (b) shows the deviation of load carrying capacity from the extrapolation of the load-strain relation in the undamaged region.

$$\text{region I: } E_{c,\mathrm{I}}A_c = E_{\mathrm{Bi}}A_{\mathrm{Bi}} + E_{\mathrm{Ag}}A_{\mathrm{Ag}} + E_{\mathrm{Alloy}}V_{\mathrm{Alloy}}, \tag{2}$$

$$\text{region II: } E_{c,\mathrm{II}}A_c = E_{\mathrm{Bi}}A_{\mathrm{Bi}} + E_{\mathrm{Alloy}}V_{\mathrm{Alloy}}, \tag{3}$$

$$\text{region III: } E_{c,\mathrm{III}}A_c = E_{\mathrm{Bi}}A_{\mathrm{Bi}}, \tag{4}$$

where the subscripts c, Bi, Ag, and Alloy refer to the composite, Bi2223, Ag, and Ag alloy, respectively. $E_{c,\mathrm{I}}A_c$, $E_{c,\mathrm{II}}A_c$, and $E_{c,\mathrm{III}}A_c$ correspond to the slopes of 0A, BC and DE in Fig. 5(a), respectively. The $E_{c,\mathrm{I}}A_c$, $E_{c,\mathrm{II}}A_c$, and $E_{c,\mathrm{III}}A_c$ values, measured from the slopes in Regions I, II and III, were 69.4, 51.7, and 34.7 kN, respectively. Substituting these measured values into Eqs. (2)–(4), we have 34.7, 17.7, and 17.0 kN for $E_{\mathrm{Bi}}A_{\mathrm{Bi}}$, $E_{\mathrm{Ag}}A_{\mathrm{Ag}}$, and $E_{\mathrm{Alloy}}A_{\mathrm{Alloy}}$, respectively. These values, together with the estimated values of yield strain (0.025%) of Ag shown below, will be used later in Sec. V for estimation of residual strain change of the constituents (Bi2223, Ag and Ag alloy) between room temperature and 77 K.

The strain at the transition from region I to II, corresponding to the yielding of Ag, was read to be 0.05% and that from region II to III, corresponding to the yielding of Ag alloy, to be 0.12%, respectively. As has been shown in Fig. 2, the sample had been cooled down from the heat-treatment temperature to 77 K (1) and had then been warmed up to room temperature RT(2) (293 K). As Ag is soft and the coefficient of thermal expansion of Bi2223 is lower than that of Ag and Ag alloy, Ag is yielded in tension at 77 K.[27] Upon warming up from 77 K (1) to RT(2), compressive stress is exerted on Ag. As shown later in detail in Sec. V, the increment in temperature of 216 K (293 K−77 K) is large enough to cause compressive yielding of Ag. Thus, at RT(2), Ag is yielded in compression. Accordingly, in region I, Ag deforms elastically from the yielded state in compression to that in tension. Noting the yield strain of Ag as $\varepsilon_{\mathrm{Ag},y}$, and approximating the Ag as an elastic-perfect plastic body where the strain hardening in the plastic deformation range is treated to be zero and the stress in the plastic deformation stage is treated to remain constant, the strain at the transition from region I to II in the stress-strain curve of the composite in Fig. 5(a) corresponds to $2\varepsilon_{\mathrm{Ag},y}$. As $2\varepsilon_{\mathrm{Ag},y}$ is read to be 0.05%, $\varepsilon_{\mathrm{Ag},y}$ is estimated to be 0.025%.

As shown later in Sec. V, Ag alloy has a residual strain 0.27% before tensile test. When the tensile strain is applied to the composite, Ag alloy deforms elastically up to the transition from region II to III (ε_T=0.12%) and then deforms plastically in region III.

In the early stage of region III, the Bi2223 filaments do not fracture. At the end of region III, they fracture, due to which the load carrying capacity of the composite is reduced in comparison with that of the composite without fracture of the filaments.[11,13,21,27,29] Figure 5(b) shows enlarged stress-strain curve of the part surrounded by the rectangle in (a). The open circle in Fig. 5(b) shows the deviation of load carrying capacity at around 0.22% strain from the extrapolation of the load-strain relation in the undamaged region. This means that the fracture of the filaments in the composite tape occurs at ε_T=0.22%. At ε_T=0%, the strain at RT(2) of the filaments along the sample length is equal to $\varepsilon_{\mathrm{Bi},r}$ (= −0.12% as shown above). Under applied tensile strain, the strain of Bi2223 becomes zero at ε_T=−$\varepsilon_{\mathrm{Bi},r}$ and, with further increasing ε_{T}, it reaches the intrinsic fracture strain $\varepsilon_{\mathrm{Bi},f}$ at ε_T=0.22%. From the value of 0.22% corresponding to $\varepsilon_{\mathrm{Bi},f}$-$\varepsilon_{\mathrm{Bi},r}$ and the value of $\varepsilon_{\mathrm{Bi},r}$=−0.12%, the $\varepsilon_{\mathrm{Bi},f}$ is estimated to be 0.10%. The estimated value is similar to the reported value of around 0.1%.[4,9,11,13,18,19,21,22,27]

IV. CRITICAL CURRENT—BENDING STRAIN RELATION IN WHICH THE BENDING STRAIN WAS GIVEN AT ROOM TEMPERATURE AND CRITICAL CURRENT WAS MEASURED AT 77 K

The shapes of the core, in which the superconducting current-transporting Bi2223 filaments are embedded in Ag, has been shown in Fig. 1(b). In the present work, the sample width direction was taken as x, the sample thickness direction as y, and the center of the sample as x=y=0, as shown in Fig. 6. The shape of the core (ABCDEFGHA in Fig. 6) was approximated by the ninth order polynomials, as follows. The length unit for x and y is mm.

$$\begin{aligned}\text{CDE in Fig. 6: } y_{\mathrm{core}} = {} & 0.066\,0214 - 0.040\,517\,3x \\ & + 1.030\,50x^2 - 4.052\,39x^3 \\ & + 8.940\,14x^4 - 12.6431x^5 + 11.3895x^6 \\ & - 6.229\,52x^7 + 1.870\,94x^8 \\ & - 0.235\,769x^9, \quad \text{for } 0 \leqslant x \leqslant 1.95,\end{aligned}$$

ABC: symmetry with EDC with respect to $x = 0$,

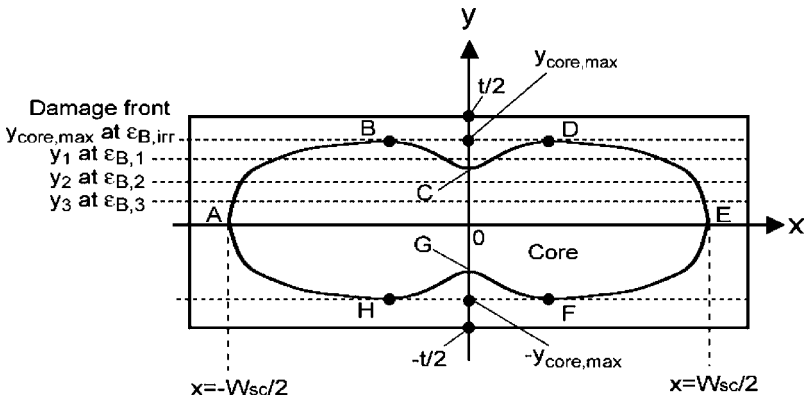

FIG. 6. Geometry of the cross section, and the definition of x and y. Under applied bending strain, the damage of the Bi2223 filaments in the core occurs first at $y_{core,max}$ when bending strain reaches $\varepsilon_{B,irr}$. For the bending strain beyond $\varepsilon_{B,irr}$, the damage front moves to y_1, y_2, and y_3 at the bending strains $\varepsilon_{B,1}$, $\varepsilon_{B,2}$, and $\varepsilon_{B,3}$, respectively.

AHGFE: symmetry with ABCDE with respect to $y=0$. (5)

In our preceding work,[29] to describe the relation of critical current to bending strain, core shape-incorporated model was presented. In the modeling, the case where the damage extends only in the region ($y>0$) above the neutral axis, was taken up. Such a model could describe the experimental results for other fabrication route—samples bent up to 1.0%. In the present work, such a model with the estimated values of $\varepsilon_{Bi,f}$ (tensile fracture strain of Bi2223 filaments) and $\varepsilon_{Bi,r}$ (residual strain) is used for prediction of critical current-bending strain relation. The predicted relation will be compared with the experimental result at the end of this section.

The relation of the geometry of the cross-section to the location of the damage front is presented in Fig. 6, where t and W_{sc} are the thickness of the composite and width of the core, respectively. The bending strain ε_B is defined as the tensile strain at the outer surface of the composite ($y=t/2$ in Fig. 6). When the sample is bent, the damage occurs first at $y_{core}=y_{core,max}$ when ε_B reaches the irreversible bending strain for critical current $\varepsilon_{B,irr}$, where $y_{core,max}$ (=0.103 mm in the present sample) is the maximum value of y_{core} [Eq. (5)], corresponding to the location of the core nearest to the outer surface of the sample. The y coordinate of the damage front, y_f, is equal to $y_{core,max}$ at $\varepsilon_B=\varepsilon_{B,irr}$, and it extends to y_1, y_2, and y_3 at $\varepsilon_B=\varepsilon_{B,1}$, $\varepsilon_{B,2}$ and $\varepsilon_{B,3}$, respectively, as shown in Fig. 6. Under the bending strain, the damage of the Bi2223 filaments is caused by the exerted tensile strain ε of the filaments along the sample length direction.[19,23,29] The tensile strain ε varies with y, and the ε-y relation varies with bending strain ε_B. Such a situation is schematically drawn in Fig. 7, in which the damage front ($y_f=y_{core,max}$, y_1, y_2, and y_3 at $\varepsilon_B=\varepsilon_{B,irr}$, $\varepsilon_{B,1}$, $\varepsilon_{B,2}$, and $\varepsilon_{B,3}$, respectively) corresponds to the geometrical situation in the cross section shown in Fig. 6. The relation among the shape of the core, bending strain, damage evolution, and critical current under bending strain is formulated as follows. The tensile strain ε of Bi2223 filaments in the sample length direction in the bent composite is expressed by $\varepsilon=\{\varepsilon_B/(t/2)\}y$.[19,29] As the Bi2223 filaments have the residual strain $\varepsilon_{Bi,r}$ (−0.12% in the present work), the total strain of the filaments is expressed by[19,29]

$$\varepsilon-\varepsilon_{Bi,r}=\{\varepsilon_B/(t/2)\}y. \quad (6)$$

Noting the intrinsic tensile fracture strain of the filaments as $\varepsilon_{Bi,f}$ and the damage front as y_f, and substituting $\varepsilon=\varepsilon_{Bi,f}$ and $y=y_f$ into Eq. (6), we have y_f as a function of ε_B in the form,

$$y_f=(\varepsilon_{Bi,f}-\varepsilon_{Bi,r})/\{\varepsilon_B/(t/2)\}. \quad (7)$$

The irreversible bending strain $\varepsilon_{B,irr}$ is calculated by substituting $y_f=y_{core,max}$ and $\varepsilon_B=\varepsilon_{B,irr}$ into Eq. (7);

$$\varepsilon_{Bi,irr}=(\varepsilon_{Bi,f}-\varepsilon_{Bi,r})/\{y_{core,max}/(t/2)\}. \quad (8)$$

With increasing ε_B beyond $\varepsilon_{B,irr}$, the damage front y_f moves to the neutral axis ($y=0$) (Figs. 6 and 7), resulting in reduction of the cross-sectional area of the current transporting Bi2223 filaments and therefore critical current. The normalized critical current, I_c/I_{c0}, where I_{c0} is the critical cur-

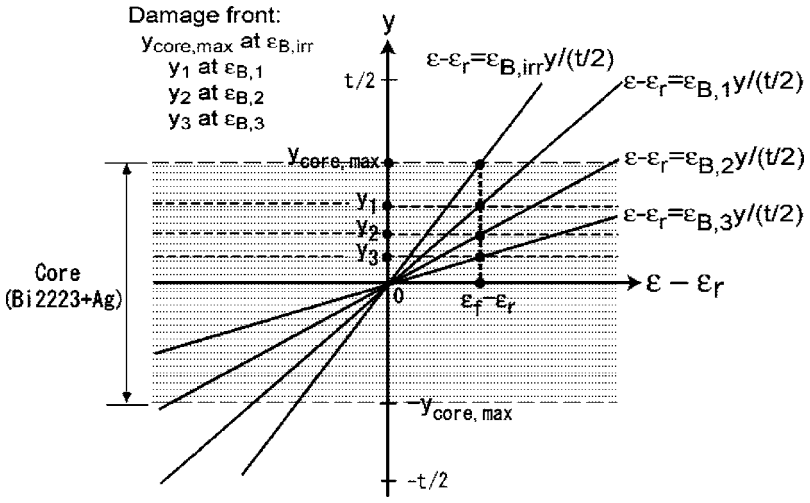

FIG. 7. Schematic representation of the relation of the damage extension to the bending strain (ε_B).

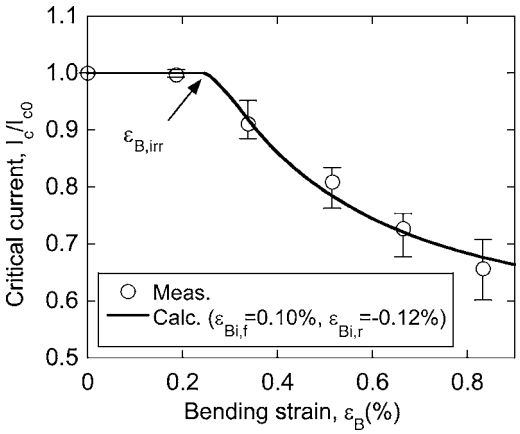

FIG. 8. Measured change of critical current I_c/I_{c0} with bending strain (ε_B), together with the calculated one (solid curve). The open circles show the average and the error bars show the maximum and minimum values measured for six test specimens. In this experiment, the specimens were bent at RT(2) and cooled down to 77 K (2), at which the critical current was measured.

rent at zero applied strain, is given by the ratio of the cross-sectional area of the surviving (undamaged) region ($-y_{\mathrm{core,max}} \leqslant y \leqslant y_f$) to that of overall core;

$$I_c/I_{c0} = 1 - 2\int_0^{W_{sc}/2} (y_{\mathrm{core}} - y_f)dx/A_{\mathrm{core}}, \tag{9}$$

where A_{core} is the cross-sectional area of the core. Substituting y_{core} [Eq. (5)] and y_f [Eq. (7)] into Eq. (9), we have

$$I_c/I_{c0} = 1 - 2\int_0^{W_{sc}/2} [y_{\mathrm{core}} - \{(\varepsilon_{Bi,f} - \varepsilon_{Bi,r}) \times (t/2)\}/\varepsilon_B]dx/A_{\mathrm{core}}, \quad \text{for } \varepsilon_B \geqslant \varepsilon_{B,\mathrm{irr}}. \tag{10}$$

For $\varepsilon_B \leqslant \varepsilon_{B,\mathrm{irr}}$, where no damage occurs, I_c/I_{c0} is 1(unity).

Figure 8 shows the measured change of I_c/I_{c0} with increasing bending strain ε_B. For $\varepsilon_B > 0.2\%$, the I_c/I_{c0} decreases with increasing ε_B. Substituting the estimated/measured values of $\varepsilon_{Bi,f}=0.10\%$, $\varepsilon_{Bi,r}=-0.12\%$, $y_{\mathrm{core,max}}=0.103$ and $t=0.23$ mm into Eq. (8), we have $\varepsilon_{B,\mathrm{irr}}=0.25\%$. Thus, $I_c/I_{c0}=1$ for $\varepsilon_B \leqslant 0.25\%$. Also substituting the estimated/measured values of $\varepsilon_{Bi,f}=0.10\%$, $\varepsilon_{Bi,f}=-0.12\%$, $W_{sc}=4.1$ mm, $A_{\mathrm{core}}=0.660$ mm^2 and y_{core} [Eq. (5)] into Eq. (10), we have I_c/I_{c0} as a function of ε_B for $\varepsilon_B \geqslant 0.25\%(\varepsilon_{B,\mathrm{irr}})$. The calculation result is presented with a solid curve in Fig. 8. The calculation result describes well the experimental result, indicating that the approach mentioned above is valid.

V. RESIDUAL STRAIN CHANGE BETWEEN ROOM TEMPERATURE AND 77 K AND IRREVERSIBLE TENSILE STRAIN FOR CRITICAL CURRENT AT 77 K

During cooling down from the heat-treatment temperature, the residual strain is accumulated in each constituent due to the difference in thermal expansion coefficient among the constituents.[4,9,10,13,15,20,21,27] The present sample had been cooled down to 77 K (1) and then heated to room temperature RT(2), at which the residual strain of Bi2223 was measured, as has been shown in Fig. 2. At RT(2), Ag had been yielded in compression, as has been shown in Sec. III. In this section, the residual strain change in the constituents (Bi2223, Ag, and Ag alloy) between RT(2) and 77 K (2) is calculated, as follows.

The residual strain $\varepsilon_{\mathrm{Alloy},r}$ of the Ag alloy at RT(2) can be estimated as follows. The residual strain $\varepsilon_{\mathrm{Bi},r}$ of Bi2223 was measured to be -0.12% at RT(2) by x-ray diffraction in Sec. III. The elastic component of the residual strain $\varepsilon_{\mathrm{Ag},r}$ at RT(2) was estimated to be $-0.025\%(=-\varepsilon_{\mathrm{Ag},y})$ from the stress-strain curve in Sec. III. The residual forces of Ag, Ag alloy, and Bi2223 are expressed by $\varepsilon_{\mathrm{Ag},r}E_{\mathrm{Ag}}A_{\mathrm{Ag}}$, $\varepsilon_{\mathrm{Alloy},r}E_{\mathrm{Alloy}}A_{\mathrm{Alloy}}$ and $\varepsilon_{\mathrm{Bi},r}E_{\mathrm{Bi}}A_{\mathrm{Bi}}$, respectively. As externally applied load is zero, the sum of the residual forces of the constituents is zero which is expressed by

$$\varepsilon_{\mathrm{Ag},r}E_{\mathrm{Ag}}A_{\mathrm{Ag}} + \varepsilon_{\mathrm{Alloy},r}E_{\mathrm{Alloy}}A_{\mathrm{Alloy}} + \varepsilon_{\mathrm{Bi},r}E_{\mathrm{Bi}}A_{\mathrm{Bi}} = 0. \tag{11}$$

Substituting the aforementioned values of $\varepsilon_{\mathrm{Ag},r}=-0.025\%$, $E_{\mathrm{Ag}}A_{\mathrm{Ag}}=17.7$ kN, $E_{\mathrm{Alloy}}A_{\mathrm{Alloy}}=17.0$ kN, $\varepsilon_{\mathrm{Bi},r}=-0.12\%$ and $E_{\mathrm{Bi}}A_{\mathrm{Bi}}=34.7$ kN into Eq. (11), we have $\varepsilon_{\mathrm{Alloy},r}=0.27\%$ at RT(2). The strain at which Ag alloy in the composite yields was 0.12%, as has been shown in Fig. 5(a). Thus, the yield strain of Ag alloy itself is 0.39%. As Young's modulus of the Ag alloy has been reported to be 88 GPa,[20] the yield stress is estimated to be around 340 MPa. This value is close to the reported value of 330 MPa estimated from the stress-strain curve.[20]

As Ag and Ag alloy have higher coefficient of thermal expansion than Bi2223 filaments, tensile strain is induced in Ag and Ag alloy during cooling and compressive one in Bi2223 filaments, while compressive strain is induced in Ag and Ag alloy and tensile one in Bi2223 filaments during heating. As Ag has low yield strain (0.025%, as has been shown in Sec. III), it is yielded in tension and in compression during cooling and heating, respectively, when the exerted strain reaches the yield strain. The change of residual strain during cooling from RT(2) to 77 K (2) is estimated as follows.

Upon cooling down from RT(2) to 77 K (2), tensile strain is induced in Ag. As Ag has been yielded in compression at RT(2) by the warming up from 77 K (1) to RT (2), the stress direction becomes reverse upon cooling down from RT(2) to 77 K (2). In such a situation, Ag deforms elastically until it comes to be yielded in tension on the way from RT(2) to 77 K (2), as shown below. Within the range where Ag deforms elastically as well as Bi2223 and Ag alloy, the coefficient of thermal expansion of the composite $\alpha_{c,\mathrm{I}}$ is expressed by Eq. (12) based on the rule of the mixtures.[4,9,13,18,23,27,28]

$$\alpha_{c,\mathrm{I}} = (\alpha_{\mathrm{Bi}}E_{\mathrm{Bi}}A_{\mathrm{Bi}} + \alpha_{\mathrm{Ag}}E_{\mathrm{Ag}}A_{\mathrm{Ag}} + \alpha_{\mathrm{Alloy}}E_{\mathrm{Alloy}}A_{\mathrm{Alloy}})/(E_{\mathrm{Bi}}A_{\mathrm{Bi}} + E_{\mathrm{Ag}}A_{\mathrm{Ag}} + E_{\mathrm{Alloy}}A_{\mathrm{Alloy}}), \tag{12}$$

where α_{Bi}, α_{Ag}, and α_{Alloy} are the coefficients of thermal expansion of Bi2223, Ag, and Ag alloy, respectively. The values of $E_{\mathrm{Bi}}A_{\mathrm{Bi}}$, $E_{\mathrm{Ag}}A_{\mathrm{Ag}}$, and $E_{\mathrm{Alloy}}A_{\mathrm{Alloy}}$ have been estimated in Sec. III. The coefficients of thermal expansion of Bi2223, Ag, and Ag alloy in the relevant temperature range are approximately given by $\alpha_{\mathrm{Bi}}=11.0\times10^{-6}/\mathrm{K}$[27] and α_{Ag}

$=\alpha_{\mathrm{Alloy}}=17.1\times10^{-6}/\mathrm{K}$.[27] Substituting these values into Eq. (4), we have $\alpha_{c,\mathrm{I}}=14.1\times10^{-6}/\mathrm{K}$.

In the range where Ag deforms elastically, the change in residual strain $\Delta\varepsilon_i$ (i=Bi2223, Ag, and Ag alloy) of each constituent for the temperature difference ΔT is given by[13,27,28]

$$\Delta\varepsilon_i=(\alpha_{c,\mathrm{I}}-\alpha_i)\Delta T \quad (i=\mathrm{Bi2223,\ Ag,\ and\ Ag\ alloy}). \tag{13}$$

As the elastic component of the residual strain of Ag at RT(2) is $-\varepsilon_{\mathrm{Ag,y}}$, the total elastic strain of Ag at a temperature T is expressed by $-\varepsilon_{\mathrm{Ag,y}}+(\alpha_{c,\mathrm{I}}-\alpha_{\mathrm{Ag}})(T-\mathrm{RT})$. When it reaches $\varepsilon_{\mathrm{Ag,y}}$ at $T=T^*$, Ag is yielded in tension. T^* is calculated by

$$T^*=2\varepsilon_{\mathrm{Ag,y}}/(\alpha_{c,\mathrm{I}}-\alpha_{\mathrm{Ag}})+\mathrm{RT}. \tag{14}$$

Substituting $\varepsilon_{\mathrm{Ag,y}}=0.025\%$, $\alpha_{c,\mathrm{I}}=14.1\times10^{-6}/\mathrm{K}$, and $\alpha_{\mathrm{Ag}}=17.1\times10^{-6}/\mathrm{K}$ into Eq. (14), we have $T^*=126$ K. The residual strain at $T=T^*$ of each constituent is calculated by

$$\varepsilon_{i,\mathrm{r},T^*}=(\alpha_{c,\mathrm{I}}-\alpha_i)(T^*-\mathrm{RT})+\varepsilon_{i,\mathrm{r}} \quad (i=\mathrm{Bi2223,\ Ag,\ and\ Ag\ alloy}), \tag{15}$$

where $\varepsilon_{\mathrm{i,r}}$ is the residual strain at RT(2).

With further cooling from T^* to 77 K (2), Ag behaves plastically. Within the range where Ag deforms plastically, the coefficient of thermal expansion of the composite $\alpha_{c,\mathrm{II}}$ is approximately given by[4,27,28]

$$\alpha_{c,\mathrm{II}}=(\alpha_{\mathrm{Bi}}E_{\mathrm{Bi}}A_{\mathrm{Bi}}+\alpha_{\mathrm{Alloy}}E_{\mathrm{Alloy}}A_{\mathrm{Alloy}})/(E_{\mathrm{Bi}}A_{\mathrm{Bi}}+E_{\mathrm{Alloy}}A_{\mathrm{Alloy}}). \tag{16}$$

Substituting the aforementioned values of α_{Bi}, α_{Alloy}, $E_{\mathrm{Bi}}A_{\mathrm{Bi}}$, and $E_{\mathrm{Alloy}}A_{\mathrm{Alloy}}$ into Eq. (16), we have $\alpha_{c,\mathrm{II}}=13.0\times10^{-6}/\mathrm{K}$. The change in residual strain of the Ag alloy and Bi2223 for the temperature difference ΔT under plastically deforming Ag is given by

$$\Delta\varepsilon_i=(\alpha_{c,\mathrm{II}}-\alpha_i)\Delta T \quad (i=\mathrm{Bi2223\ and\ Ag\ alloy}). \tag{17}$$

The total strain of Ag under plastic deformation is the sum of the elastic strain $\varepsilon_{\mathrm{Ag,elast}}$ and plastic one $\varepsilon_{\mathrm{Ag,plast}}$. Under the approximation of Ag as an elastic-perfect plastic body where the strain hardening in the plastic deformation range is treated to be zero and the stress in the plastic deformation stage is treated to remain constant, only the elastic component $\varepsilon_{\mathrm{Ag,elast}}$ in the total strain is responsible for the load carrying capacity of Ag. The elastic component of residual strain of Ag, $\varepsilon_{\mathrm{Ag,r}}$, under tensile plastic deformation is given by $+\varepsilon_{\mathrm{Ag,y}}$. The residual strain at $T=77$ K (2) is calculated by

$$\varepsilon_{\mathrm{Ag,r},77(2)}=+\varepsilon_{\mathrm{Ag,y}},\quad \varepsilon_{i,\mathrm{r},77(2)}=(\alpha_{c,\mathrm{II}}-\alpha_i)(77-T^*)+\varepsilon_{i,\mathrm{r},T^*} \quad (i=\mathrm{Bi2223\ and\ Ag\ alloy}), \tag{18}$$

where T^* is 126 K as stated above. The calculated changes of the residual strain value of the constituents during cooling from RT(2) to 77 K (2) are presented in Fig. 9.

As shown in Fig. 9, the residual strain of Bi2223 filaments at 77 K was calculated to be −0.18%. The intrinsic

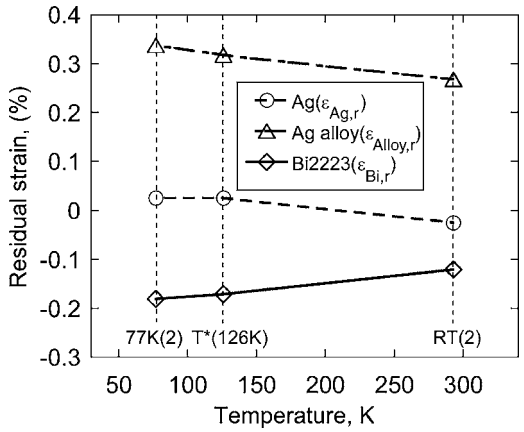

FIG. 9. Calculated residual strain change of each constituent during cooling from RT(2) to 77 K (2).

fracture strain of Bi2223 filaments at room temperature of the present sample was estimated to be 0.1%, as has been shown in Sec. III. Assuming the intrinsic fracture strain at 77 K is same as that at RT, the fracture strain of Bi2223 embedded in the composite at 77 K, $\varepsilon_{\mathrm{Bi,f}}-\varepsilon_{\mathrm{Bi,r}}$, corresponding to the irreversible tensile strain $\varepsilon_{T,\mathrm{irr}}$ of the composite at which the critical current starts to be reduced by the fracture of the filaments, was predicted to be 0.28%.

In order to examine whether the critical current is actually reduced at such a predicted irreversible strain value or not, the change of the critical current I_c was measured at 77 K as a function of applied tensile strain ε_T for two specimens. Figure 10 shows the result, in which the critical current I_c is normalized with respect to that of the sample under no applied strain, I_{c0}, as similarly as that for bending (Fig. 8). Concerning the I_c/I_{c0}-ε_T relation, it has been known that the I_c/I_{c0} value decreases linearly with increasing ε_T due to the intrinsic strain dependence of the critical current.[11,21] The empirical relation I_c/I_{c0} to ε_T for $\varepsilon_T\leqslant\varepsilon_{T,\mathrm{irr}}$ has been derived to be[21]

$$I_c/I_{c0}=1-0.09\varepsilon_T(\varepsilon_T:\%). \tag{19}$$

With Eq. (19), the measured I_c/I_{c0}-ε_T relation for three different fabrication route samples[11] has commonly been de-

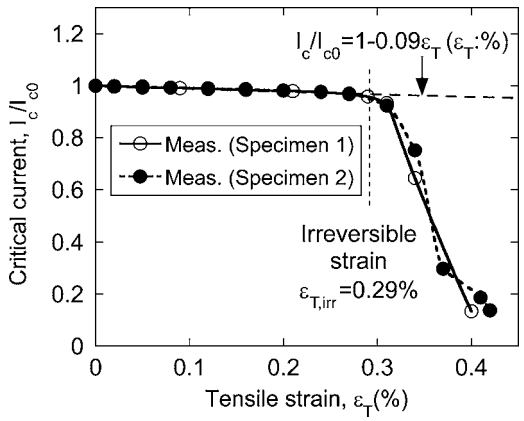

FIG. 10. Measured change of the normalized critical current I_c/I_{c0} with increasing applied tensile strain ε_T on composite and estimated irreversible strain $\varepsilon_{T,\mathrm{irr}}$. In this experiment, the samples were pulled in tension at 77 K and the critical current was successively measured at the same temperature.

scribed well.[21] The present result up to ε_T=0.29% was also described by Eq. (19) and the result beyond 0.29% deviated from the extrapolation of Eq. (19), as shown in Fig. 10. Thus, 0.29% was identified as the irreversible tensile strain $\varepsilon_{T,\mathrm{irr}}$ in the present sample, which was close to the predicted value of 0.28%.

It is noted that the fracture strain of filaments is not unique, being different to each other.[30] Accordingly, filaments are not fractured simultaneously and I_c/I_{c0} does not drop suddenly, as shown in Fig. 10. However, the severe reduction in I_c/I_{c0} occurs within a limited small strain range under tensile applied strain [I_c/I_{c0} goes down to around 0.5 by 0.05% tensile strain increment after the irreversible strain (Fig. 10)]. On the other hand, under the bending strain, the I_c/I_{c0} goes down rather gradually in wide strain range [it goes down to around 0.65 by 0.6% bending strain increment after the irreversible strain (Fig. 8)]. The gradual decrease in I_c/I_{c0} under the bending applied strain stems from the gradual extension of damage front with increasing strain, as has been shown in Sec. IV.

It was shown in the present work that the change of critical current at 77 K by bending at room temperature and tensile irreversible strain for critical current at 77 K under applied tensile strain at 77 K can be predicted from the measurement of residual strain of Bi2223 filaments and stress-strain curve of the composite tape at room temperature. The present approach is simple and applicable to any fabrication-route samples, being a useful tool for prediction of critical current change of filamentary conductors under tensile and bending strains.

VI. CONCLUSIONS

(1) An estimation method of residual and fracture strains of Bi2223 filaments at room temperature and 77 K, which uses tensile test, x-ray diffraction measurement, and modeling analysis, and a prediction method of critical current change under tensile and bending strains using the estimated residual and fracture strains of the filaments were presented.

(2) The residual strain of Bi2223 filaments in the composite tape at room temperature was estimated to be −0.12% by the x-ray diffraction method. The intrinsic fracture strain of Bi2223 filaments was estimated to be 0.1% from the analysis of load-strain curve in combination with the residual strain value. With these values, the measured change of critical current measured at 77 K as a function of bending strain applied at room temperature was described well.

(3) The changes of residual strain of Bi2223 filaments, Ag, and Ag alloy in the composite tape during cooling from room temperature to 77 K were calculated as a function of temperature with the rule of mixtures. The calculated residual strain of Bi2223 at 77 K and the intrinsic fracture strain estimated in (2) predicted the irreversible tensile strain for critical current at 77 K to be 0.28%, which was very close to the experimental value of 0.29%.

ACKNOWLEDGMENTS

The present work was supported by the grant-in-aid of The Ministry of Education, Culture, Sports, Science and Technology, Japan (No. 18106011).

[1] P. Vase, R. Flükiger, M. Leghissa, and B. Glowacki, Supercond. Sci. Technol. **13**, R71 (2000).
[2] H. Kitaguchi, K. Itoh, H. Kumakura, T. Takeuchi, K. Togano, and W. Wada, IEEE Trans. Appl. Supercond. **11**, 3058 (2001).
[3] H. J. N. van Eck, K. Vargast, B. ten Haken, and H. H. J. ten Kate, Supercond. Sci. Technol. **15**, 1213 (2003).
[4] S. Ochiai, K. Hayashi, and K. Osamura, Cryogenics **33**, 976 (1993).
[5] R. Wesche, A. M. Fuchs, K. Jakob, and G. Pasztor, Cryogenics **36**, 419 (1996).
[6] B. ten Haken, A. Godeke, H.-J. Schluver, and H. ten Kate, Adv. Cryog. Eng. **42**, 651 (1997).
[7] B. ten Haken, A. Beuink, and H. ten Kate, IEEE Trans. Appl. Supercond. **7**, 2034 (1999).
[8] R. T. Aloysius, A. Sobha, P. Guruswamy, and U. Samaprasad, Supercond. Sci. Technol. **14**, 85 (2001).
[9] R. Passerini, M. Dhalle, E. Giannini, G. Witz, B. Seeber B, and R. Flükiger, Physica C **371**, 173 (2002).
[10] R. Passerini, M. Dhalle, B. Seeber, and R. Flükiger, Supercond. Sci. Technol. **15**, 1507 (2002).
[11] K. Osamura, M. Sugano, and K. Matsumoto, Supercond. Sci. Technol. **16**, 971 (2003).
[12] S. J. Sun, W. Liu, X. P. Chen, M. Y. Li, and Z. Han, Supercond. Sci. Technol. **16**, 984 (2003).
[13] S. Ochiai, T. Nagai, H. Okuda, S. S. Oh, M. Hojo, M. Tanaka, M. Sugano, and K. Osamura, Supercond. Sci. Technol. **16**, 988 (2003).
[14] K. Katagiri, H. S. Shin, K. Kasaba, T. Tsukinokizawa, K. Hiroi, T. Kuroda, K. Itoh, and H. Wada, Supercond. Sci. Technol. **16**, 995 (2003).
[15] H. S. Shin and K. Katagiri, Supercond. Sci. Technol. **16**, 1012 (2003).
[16] H. J. N. van Eck, D. C. van der Laan, M. Dhallé, B. ten Haken, and H. H. J. ten Kate, Supercond. Sci. Technol. **16**, 1026 (2003).
[17] A. Nyilas, K. Osamura, and M. Sugano, Supercond. Sci. Technol. **16**, 1036 (2003).
[18] M. Hojo, M. Nakamura, T. Matsuoka, M. Tanaka, S. Ochiai, M. Sugano, and K. Osamura, Supercond. Sci. Technol. **16**, 1043 (2003).
[19] S. Ochiai, N. Miyazaki, D. Doko, T. Nagai, M. Nakamura, H. Okuda, S. S. Oh, M. Hojo, M. Tanaka, and K. Osamura, J. Nucl. Mater. **329–333**, 1585 (2004).
[20] M. Sugano, K. Osamura, and A. Nyilas, Physica C **412–414**, 1114 (2004).
[21] S. Ochiai, T. Ishida, D. Doko, K. Morishita, H. Okuda, S. S. Oh, D. W. Ha, M. Hojo, M. Tanaka, M. Sugano, and K. Osamura, Supercond. Sci. Technol. **18**, S232 (2005).
[22] M. Hojo, M. Nakamura, M. Tanaka, T. Adachi, M. Sugano, S. Ochiai, and K. Osamura, Supercond. Sci. Technol. **18**, S356 (2005).
[23] A. Otto, E. J. Harley, and R. Marson, Supercond. Sci. Technol. **18**, S308 (2005).
[24] A. Nyilas, Supercond. Sci. Technol. **18**, S409 (2005).
[25] T. Kuroda, K. Itoh, K. Katagiri, W. Goldacker, W. Haessler, B. ten Haken, M. Kiuchi, N. Noto, S. Ochiai, S. Otabe, H. S. Shin, J. Sosnowski, H. Weijers, H. Wada, and K. Kumakura, Physica C **425**, 111 (2005).
[26] K. Katagiri, T. Kuroda, H. S. Shin, K. Hiroi, K. Itoh, and H. Wada, Physica C **426–431**, 1200 (2005).
[27] S. Ochiai, H. Rokkaku, K. Morishita, J. K. Shin, S. Iwamoto, H. Okuda, M. Hojo, K. Osamura, M. Sato, A. Otto, E. Harley, and A. Malozemoff, Supercond. Sci. Technol. **20**, 202 (2007).
[28] D. K. Hale, J. Mater. Sci. **11**, 2105 (1976).
[29] S. Ochiai, T. Matsuoka, J. K. Shin, H. Okuda, M. Sugano, M. Hojo, and K. Osamura, Supercond. Sci. Technol. **20**, 1076 (2007).
[30] S. Ochiai, T. Ishida, D. Doko, K. Morishita, H. Okuda, S. S. Oh, D. W. Ha, M. Hojo, M. Tanaka, M. Sugano, and K. Osamura, Supercond. Sci. Technol. **18**, S356 (2005).